Biochemical and Biophysical Research Communications 455 (2014) 246–250

Contents lists available at ScienceDirect

Biochemical and Biophysical Research Communications

journal homepage: www.elsevier.com/locate/ybbrc

Improved tumor-targeting MRI contrast agents: Gd(DOTA) conjugates of a cycloalkane-based RGD peptide

Ji-Ae Park [a,1], Yong Jin Lee [a], In Ok Ko [a], Tae-Jeong Kim [b], Yongmin Chang [b], Sang Moo Lim [c], Kyeong Min Kim [a,*], Jung Young Kim [a,*]

[a] Molecular Imaging Research Center, Korea Institute of Radiological & Medical Sciences, Seoul, Republic of Korea
[b] Institute of Biomedical Engineering, Kyungpook National University, Daegu, Republic of Korea
[c] Department of Nuclear Medicine, Korea Institute of Radiological & Medical Sciences, Seoul, Republic of Korea

ARTICLE INFO

Article history:
Received 27 October 2014
Available online 6 November 2014

Keywords:
Cyclic RGD peptide
Tumor targeting
MRI
Contrast agents
Gd-DOTA

ABSTRACT

Two new MRI contrast agents, Gd-DOTA-c(RGD-ACP-K) (**1**) and Gd-DOTA-c(RGD-ACH-K) (**2**), which were designed by incorporating aminocyclopentane (ACP)- or aminocyclohexane (ACH)-carboxylic acid into Gd-DOTA (gadolinium-tetraazacyclo dodecanetetraacetic acid) and cyclic RGDK peptides, were synthesized and evaluated for tumor-targeting ability *in vitro* and *in vivo*. Binding affinity studies showed that both **1** and **2** exhibited higher affinity for integrin receptors than cyclic RGDyK peptides, which were used as a reference. These complexes showed high relaxivity and good stability in human serum and have the potential to improve target-specific signal enhancement *in vivo* MR images.

1. Introduction

Magnetic resonance imaging (MRI) is a powerful technique for the medical diagnosis of tumors, providing excellent anatomy images based on the assistance of contrast agents (CAs) that catalytically shorten the relaxation time of the nearby water molecules [1–3]. One of the most important issues in the development of the targeted MRI CAs is the lower sensitivity of CA detection in comparison to the diagnostic techniques used in nuclear medicine. To achieve high signal enhancement of a target site with MRI CAs, the CAs must either exhibit very high relaxivity or contain nanomaterials with superior gadolinium (Gd) loading capabilities [4–6]. Although macromolecular CAs demonstrate increased contrast enhancement, they do not display significantly improved tumor-targeting due to their limited *in vivo* biodistribution. Namely, one study reports that less than 5% of a nanoplatform-based molecule reaches the target site after intravenous injection, while the remainder is taken up by the reticuloendothelial system (RES) [7]. In contrast, targeted small molecule CAs offer the advantage of being rapidly cleared from the blood, resulting in adequate tumor/blood ratios at earlier times. Other advantages of small molecule CAs include the reproducible synthesis of high purity products and reduced immunogenicity, which is important for clinical translation. Additionally, the accumulation of targeted CAs on tumor cells could overcome the disadvantages of many small molecules with low sensitivity. The design of targeted CAs is necessary to maintain high relaxivity and high tumor affinity. To increase the targeting ability of CAs based on small molecules, the conjugation of cyclic RGD (Arg-Gly-Asp) peptides is one of the best strategies. We previously reported Gd complex of DOTA-RGD conjugate for use as an MRI CAs for αvβ3 integrin imaging [8].

Cyclic RGD (Arg-Gly-Asp) peptides, which bind to αvβ3 integrin receptors that are over-expressed in nascent endothelial cells during angiogenesis in various tumor types, commonly used BAMs (biologically active molecules) in the tumor-targeting image agents [9–11]. Consequently, a large number of RGD derivatives have been developed in an effort to improve not only the pharmacokinetics but also the binding affinity toward specific integrin receptors [12–14]. In a previous study, Casiraghi designed a series of RGD-based semi peptides containing monocyclic and bicyclic turn-inducing motifs *via* structural modifications to the develop high affinity conformations [15,16]. Cyclic RGD peptides containing of a γ-aminocyclopentane carboxylic acid (Acpca) exhibited superior binding efficiency. Based on these results, we aimed to develop highly efficient tumor-targeted MRI CAs using cycloalkane-based cyclic RGD peptides. More recently, we reported two novel cycloalkane-based cyclic RGD peptides, c(RGD-ACP-K) and

* Corresponding authors at: Molecular Imaging Research Center, Korea Institute of Radiological & Medical Sciences, 75 Nowon-gil, Nowon-Gu, Seoul 139-706, Republic of Korea. Fax: +82 2 970 1341 (J.Y. Kim).
E-mail addresses: jpark@kirams.re.kr (J.-A. Park), jykim@kirams.re.kr (J.Y. Kim).
[1] Address: Molecular Imaging Research Center, Korea Institute of Radiological & Medical Sciences, 75 Nowon-gil, Nowon-Gu, Seoul 139-706, Republic of Korea. Fax: +82 2 970 1341.

http://dx.doi.org/10.1016/j.bbrc.2014.10.155
0006-291X/

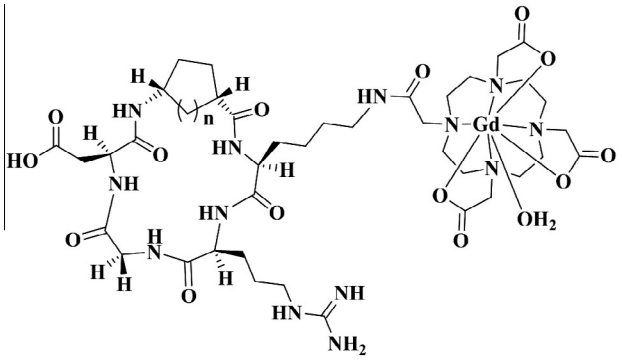

(1) n=1, ACP; (1S, 3R)-3-aminocyclopentane-1-carboxylic acid

(2) n=2, ACH; (1S, 3R)-3-aminocyclohexane-1-carboxylic acid

Chart 1.

c(RGD-ACH-K), which incorporated aminocyclopentane (ACP) and aminocyclohexane (ACH) carboxylic acids, respectively, and exhibited high affinity toward U87MG glioblastoma cells [17].

Consistent with these efforts and as part of our continued search for Gd-based MRI CAs, we introduce two cycloalkane-based RGD peptides conjugated with DOTA (1,4,7,10-tetraaqacyclododecane-1,4,7,10-tetraacetic acid) for the chelation of Gd: Gd-DOTA-c(RGD-ACP-K) (**1**) and Gd-DOTA-c(RGD-ACH-K) (**2**) (Chart 1). The tumor-targeting properties and imaging potential of **1** and **2** were evaluated *in vitro* and *in vivo*.

2. Materials and methods

All reagents were purchased from commercial sources and used as received. Solvents were purified and dried using standard procedures. Fmoc-L(D)-Amino acids, reagents (DIC, HOBt, HOAt) were purchased from Novabiochem and 1,4,7,10-Tetraazacyclododecane-1,4,7,10-tetraacetic acid (DOTA) obtained from Macrocyclics, Inc. (Dallas, Tx). (1S,3R)-Fmoc-3-aminocyclopnetane-1-carboxylic acid was purchased from Anaspec (San Jose, CA, USA) and Fmoc-cis-1,3-aminocyclohexane carboxylic acid was purchased from Santa Cruz biotechnology, Inc. The c(RGD) peptide, c(RGD-ACP-K) and c(RGD-ACH-K), were custom synthesized by Anygen, Inc. (Korea) using the PIT-Symphony peptide synthesizer by the standard Fmoc (9-fluorenylmethoxy-carbonyl) methodology, as described previously [18,19].

2.1. c(RGD-ACP-K)-DOTA-Gd (*1*) and c(RGD-ACH-K)-DOTA-Gd (*2*)

For the formation of **1**, c(RGD-ACP-K)-DOTA conjugate was initially prepared as follows: To a solution of c(RGD-ACP-K) (5 mM) and DOTA (10 mM) in DMSO (250 mL), were added HOBt (20 mM) in DIC (20 mM). The mixture was then stirred at RT for 24 h. The formation of c(RGD-ACP-K)-DOTA conjugate was confirmed by Waters HPLC system equipped with a C_{18} analytical column (5 μm, 3.0 × 150 mm) with the following separation conditions: A mixture of an aqueous solution of solvent A (0.1% TFA in acetonitrile) and solvent B (0.1% TFA in water) with a 30 min linear gradient (from 5% to 40%) at a flow rate of 0.43 mL/min; retention time (R_t) = 7.4 min; MALDI-TOF-MS: m/z = 953.5 ($C_{40}H_{67}N_{13}O_{14}$, Calculated MW = 954.0). An aqueous solution of $GdCl_3{\cdot}6H_2O$ (25 mM) and c(RGD-ACP-K)-DOTA (25 mM) in H_2O (450 mL) was prepared to be stirred for 48 h at 40 °C. The formation of **1** was confirmed by HPLC with the same condition above; R_t (**1**) = 8.1 min. MALDI-TOF-MS: m/z = 1110.5 ($C_{40}H_{67}GdN_{13}O_{14}$, Calculated MW = 1111.3). The solution was lyophilized and purified by preparative C18 column (10 μm, 25 × 250 mm) with the same mobile phase above with a flow rate of 8 mL/min.

For the formation of **2**, the compound was prepared as described above by replacing c(RGD-ACP-K)-DOTA with c(RGD-ACH-K)-DOTA. R_t (c(RGD-ACH-K)-DOTA) = 9.2 min; MALDI-TOF-MS: m/z = 967.7 ($C_{41}H_{69}N_{13}O_{14}$, Calculated MW = 967.5). R_t (**2**) = 9.8 min. MALDI-TOF-MS: m/z = 1122.3 ($C_{41}H_{66}GdN_{13}O_{14}$, Calculated MW = 1122.2).

2.2. In vitro stabilities of *1* and *2*

The stabilities were monitored by analytical HPLC on a Waters 515 temary pump with UV detection. The typical protocol is as follows: To human serum (950 μL) was added **1** or **2** (10 mM, 50 μL), and the mixture was placed in an incubator at 37 °C at different intervals (0, 0.5, 1, 2, 4, 6, 24 and 72 h). Aliquots of serum (70 μL) were treated with EtOH (140 μL) for protein precipitation. Samples were centrifuged at 13,200 rpm for 10 min at 4 °C. The supernatant solution was collected and passed through a Millex GV filter (0.22 μm), and the degree of stability detected by UV absorbance at 200 nm. Atlantis dC-18 column (3.0 × 150 mm) with the mobile phase 5% solvent A (0.1% TFA in acetonitrile) and 40% solvent B (0.1% TFA in water) with a flow rate of 0.43 mL/min was used as elution condition.

2.3. Cell binding assay

The receptor-binding assay of the **1** and **2** were compared with Gd-DOTA-RGD and c(RGDyK) (reference molecules) using ^{125}I-echistatin on U87MG cells as described previously [20,21]. U87MG cells (2×10^6/100 μL) were resuspended in binding buffer (DMEM complemented with 1% BSA, 1 mM $MnCl_2$, 1 U/mL penicillin G, and 1 μg/mL streptomycin). For the assay, equal volumes of nonradioactive ligands **1**, **2**, Gd-DOTA-RGD, c(RGDyK) and radioactive ligand (^{125}I-echistatin, 0.1 μCi) were added. Increased concentrations (10^{-4} to 10^{-12} M) of the ligands were added to consecutive wells. The plates were incubated for 40 min at 37 °C and then the reaction medium was removes and the cells were washed three times with PBS. The cells were harvested and the bound ^{125}I-echistatin was counted in a gamma counter, 1480 WIZARD (WALLAC). Data was analyzed with GraphPad Prism 5 software to determine the IC_{50} value.

2.4. Relaxivity measurements

T_1 measurements were carried out using an inversion recovery method with a variable inversion time (TI) at 3 T (128 MHz, Magnetom Trio Tim, Siemens). The MR images were acquired at 35 different TI values ranging from 50 to 1750 ms. T_1 relaxation times were obtained from the non-linear least square fit of the signal intensity measured at each TI value. For T_2 measurements, the CPMG (Carr-Purcell-Meiboon-Gill) pulse sequence was adapted for multiple spin-echo measurements. Thirty-four images were acquired with 34 different echo time (TE) values ranging from 10 to 1900 ms. T_2 relaxation times were obtained from the non-linear least squares fit of the mean pixel values for the multiple spin-echo measurements at each echo time. Relaxivities (R_1 and R_2) were then calculated as an inverse of relaxation time per mM.

2.5. Tumor xenograft model

Animal procedures were performed according to a protocol approved by the animal research committee of Korea Institute of Radiological and Medical Sciences (KIRAMS). Female BALB/c nude mice (SLC, Hamamatsu, Japan) at 4–6 weeks of age, were injected subcutaneously in the left arm with 5×10^6 U87MG glioblastoma

Table 1
The relaxation data for 1, 2, Gd-DOTA-RGD[a] and Dotarem at 128 MHz and 298 K.

	R_1 (mM^{-1} s^{-1})	R_2 (mM^{-1} s^{-1})
1	5.1 ± 0.1	5.7 ± 0.1
2	5.5 ± 0.1	5.6 ± 0.1
Gd-DOTA-RGD	6.5 ± 0.1	6.8 ± 0.2
Dotarem	3.7 ± 0.1	4.6 ± 0.1

[a] Compound obtained from Ref. [8].

cells suspended in 100 μL Dulbecco's modified eagle's medium (DMEM). The mice were subjected to biodistribution and SPECT/MRI studies when the tumor volume reached 5–7 mm in diameter (10–14 day after implant).

2.6. In vivo MR imaging

Whole-body MR images were taken with a 3 T MR unit (Magnetom Trio Tim, Siemens) with an animal coil. The mice were anesthetized with 1.5% isoflurane in oxygen and images acquired before and after injection of **1**, **2** or Dotarem (0.1 mmol/kg) via tail vein. The T1-weighetd fast spin-echo imaging was performed under the following condition: repetition time = 9.9 ms; echo time = 3.2 ms; 10 mm field of view; 256 × 205 matrix size; 1 mm slice thickness; average = 3. In addition, to evaluate the specificity of tumor targeting of complexes, we performed receptor-blocking experiments. In blocking experiment, tumor bearing mice were initially injected with c(RGDYK) (5 mg) and subsequently after 40 min, MR images were obtained with injection of **1** or **2** (0.1 mmol/kg).

The signal-to-noise ratio (SNR) is defined as the ratio of mean signal intensity the anatomic resions of interest (ROI) to that of the background noise. The contrast-to-noise ratio (CNR) is defined as the difference in SNR between adjacent anatomic structures.

$$CNR = SNR_{after} - SNR_{before}$$

The Normalized signal was calculated as follows:

$$\text{Normalized signal} = CNR/CNR_{max} \times 100$$

3. Results and discussion

The synthesis of the cycloalkane-based cyclic RGD peptides, c(RGD-ACP-K) and c(RGD-ACH-K), was accomplished using modifications of previously described methods [8]. Briefly, solid-phase peptide synthesis (SPPS) was carried out on a PIT-Symphony peptide synthesizer using an Fmoc (9-fluorenylmethoxy-carbonyl) methodology [22]. Activated Fmoc-protected amino acids were required by the instrument protocol. The activation was performed by combining 1-hydroxybensotriazole (HOBt) and dichloromethane (DIC). In each complex, either ACP or ACH was inserted into the corresponding c(RGDK), resulting in c(RGD-ACP-K) or c(RGD-ACH-K), respectively. The DOTA-containing conjugates, c(RGD-ACP-K)-DOTA and c(RGD-ACH-K)-DOTA, were prepared such that DOTA was attached to the L-lysine (K) side chains. The Gd complexes, **1** and **2**, were prepared by treating the conjugates with $GdCl_3 \cdot 6H_2O$ in water. The final product was isolated after purification by reverse-phase HPLC, and the complex formation was confirmed by MALDI-mass spectroscopy (see ESI for the HPLC data and mass data).

Table 1 shows the proton relaxivities, R_1 and R_2, of **1** and **2** along with Dotarem (Gd-DOTA) and Gd-DOTA-RGD [8] for comparative purposes. The relaxivities of **1** and **2** are more than 1.5 times as high as that of Dotarem, which may be explained by slower molecular tumbling as a result of the increase in molecular weight achieved through conjugation with cyclic RGD peptides [2]. Moreover, the R_1 value of Gd-DOTA-RGD is slightly higher than that of **1** and **2** for the same reason.

Both **1** and **2** exhibited high stability in human serum for 3 days at 37 °C, demonstrating kinetic inertness toward degradation by endogenous enzymes. Fig. 1 shows the *in vitro* serum stability of **1** as a function of time, as measured by monitoring the UV absorbance at 200 nm using an HPLC system. The **1** eluted at 8.1 min (Fig. S3) was assigned by comparison to a known molecular weight standard. No peak corresponding to c(RGD-ACP-K)-DOTA (R_t, 7.4 min; Fig. S1) dissociated from **1** was observed in 3 days of incubation. (see ESI for *in vitro* serum stability of **2**).

We compared the receptor-binding affinity of **1**, **2**, Gd-DOTA-RGD and c(RGDyK) using a competitive cell-binding assay

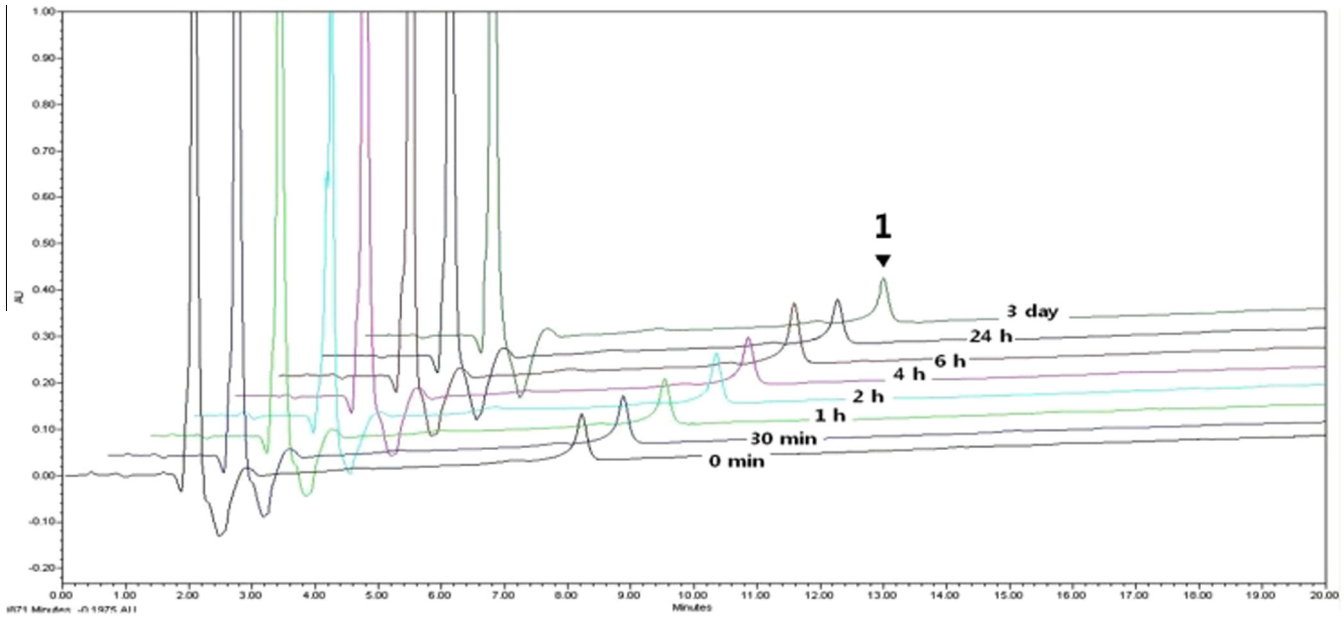

Fig. 1. HPLC spectra of **1** incubated in human serum at 37 °C at different time intervals.

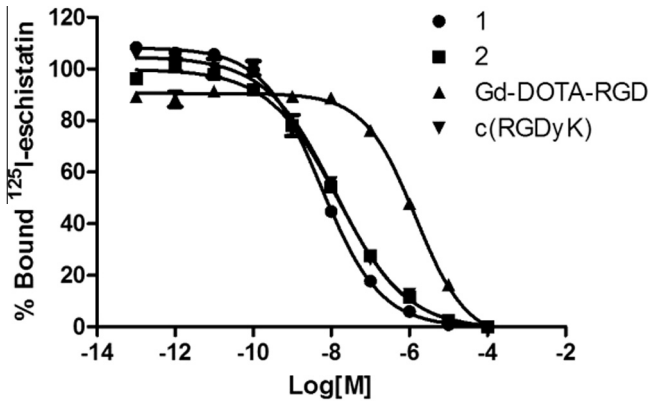

Fig. 2. Inhibition of ^{125}I-eschistatin binding to integrin $\alpha_v\beta_3$ on U87MG cells by **1**, **2**, Gd-DOTA-RGD and c(RGDyK) (n = 3, means ± SD).

method. All peptide conjugates inhibited the binding of ^{125}I-echistatin to U87MG cells in a concentration dependent manner [23]. Both **1** and **2** demonstrated significantly higher affinities, compared with Gd-DOTA-RGD; the calculated IC_{50} values for **1**, **2**, Gd-DOTA-RGD and c(RGDyK) were 5.5 ± 0.3, 15.0 ± 2.0, 1447 ± 284 and 12.4 ± 1.5 nM, respectively (Fig. 2). Notably, the introduction of an ACH/ACP moiety significantly increased the binding affinity. These results may be explained in part by the difference in conformational rigidity between the amino cycloalkane derivatives (ACH/ACP). The binding affinity of cyclic RGD peptides depends not only on the stereochemistry of the individual amino acids but also on the conformation of the overall cyclic backbone [15].

The *in vivo* tumor targeting ability of **1** was examined using a U87MG glioblastoma xenograft model, which is well known to exhibit high integrin $\alpha v\beta 3$ expression [24,25]. For MR imaging in the targeting experiments, the anesthetized animals were injected with **1** at a dosage of 0.1 mmol/kg *via* the tail vein, and T1-weighted images were acquired over 480 min (n = 3). The pre- and post-injection MR images in Fig. 3A and B, respectively, shows a significant signal enhancement in the tumor after injection. The specificity of tumor targeting can be further validated by receptor-blocking experiments. For the blocking study, c(RGDyK) was injected at 40 min after the injection of **1**, and MR images were obtained using the same protocols described above. The signal intensity of the tumor was reduced significantly, as demonstrated by Fig. 3C and D. The degree of signal difference with **1**, as expressed by the contrast-to-noise ratio (CNR), was approximately 20% higher than that obtained from the blocking experiments, as shown in Fig. 3E. This result clearly demonstrates that **1** is capable of specifically targeting the $\alpha_v\beta_3$ integrin expressed on the tumor cells (see ESI for the *in vivo* MR images of **2**). The target-specific nature of **1** may be further confirmed by comparing the normalized signal intensity of **1** as a function of time with that of Dotarem. Fig. 3F shows that the signal intensity of Dotarem exhibited a rapid increase, with the start of excretion within 20 min, while the signal intensity of **1** demonstrated a significant increase for up to 40 min after injection and persisted for 120 min. Consistent with the blocking experiment data, this result demonstrated that both **1** and **2** are efficient tumor-targeting MRI CAs for $\alpha_v\beta_3$ integrin.

An additional advantage of **1** and **2**, compared with Gd-DOTA-RGD, is the incorporation of cycloalkane derivatives as non-natural amino acids [15,16,26] rather than natural amino acids into the cyclic RGD peptide sequence. Thus, an increase in binding affinity would be expected with **1** and **2** in comparison

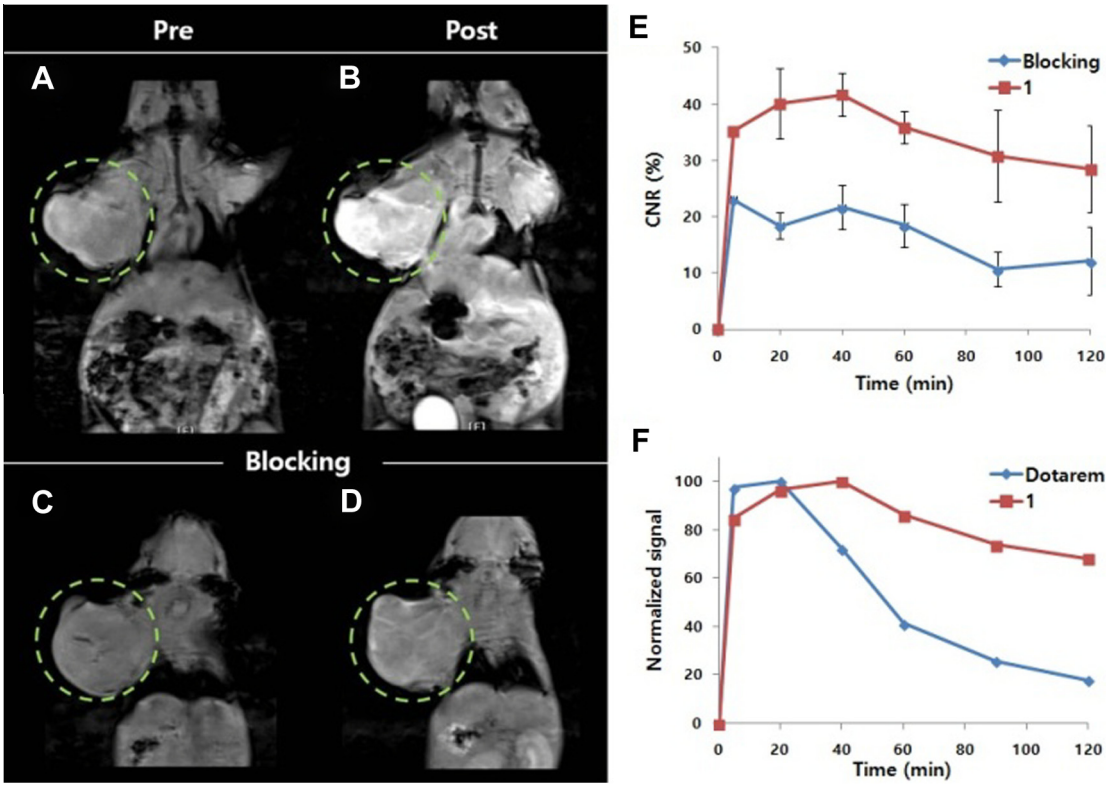

Fig. 3. *In vivo* MR images of mice with U87MG tumor cells obtained from the **1** (A and B) and blocking (C and D) experiments; the contrast-to-noise ratio (CNR) of the tumor as a function of time in the **1** (■) and blocking (♦) experiments (E); The normalized signal intensities of the tumor as a function of time measured from the MR images with **1** (■) and Dotarem (♦) (F).

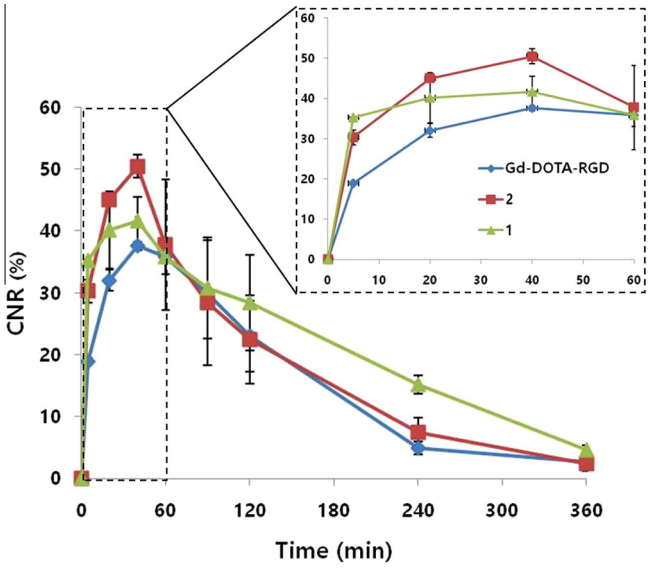

Fig. 4. The CNR profiles of the tumor as a function of time obtained with **1** (▲), **2** (■) and Gd-DOTA-RGD (♦).

to Gd-DOTA-RGD. This expectation is demonstrated in Fig. 4, which shows the CNR as a function of time for various MRI CAs. Although the relaxivities of **1** and **2** are lower than that of Gd-DOTA-RGD, the degree of signal enhancement with **1** and **2** is higher than that with Gd-DOTA-RGD within 60 min. Consequently, the slow *in vivo* metabolism observed for complex **1** over 360 min, compared with the corresponding Gd-DOTA-RGD complex, may be rationalized in terms of the stereochemistry cited above [15,16,26].

The enhanced signal in the kidney and bladder indicates that the CAs was excreted through renal. No apparent side effects were observed during the *in vivo* mice experiments, and all animals survived for more than a few months after the experiment.

In summary, this work describes the successful synthesis and application of **1** and **2** as potential tumor targeted MRI CAs. These complexes demonstrated not only improved affinity for $\alpha_v\beta_3$ integrin but also higher R_1 relaxivity. Future efforts include the elucidation and optimization of the mechanisms through which **1** and **2** bind to integrin and their potential applications for specific imaging of integrin.

Acknowledgments

This work was partially supported by the Programs of Development Research Center of PET Application Technology and the programs of Clinical Application Research of Radiopharmaceuticals in the National Nuclear Technology Program, Republic of Korea (ROK). The work was also partially supported by the Nuclear R&D Program (Grant No. 2012013722) through the National Research Foundation of Korea (NRF) funded by the Ministry of Science, ICT & Future Planning, ROK.

Appendix A. Supplementary data

Supplementary data associated with this article can be found, in the online version, at http://dx.doi.org/10.1016/j.bbrc.2014.10.155.

References

[1] P. Caravan, J.J. Ellison, T.J. McMurry, R.B. Lauffer, Chem. Rev. 99 (1999) 2293–2352.
[2] P. Caravan, Chem. Soc. Rev. 35 (2006) 512–523.
[3] E. Terreno, W. Dastrù, D. Delli Castelli, E. Gianolio, S. Geninatti Crich, D. Longo, S. Aime, Curr. Med. Chem. 17 (2010) 3684–3700.
[4] M. Tan, Z.R. Lu, Theranostics 1 (2011) 83–101.
[5] C.A. Boswell, P.K. Eck, C.A. Regino, M. Bernardo, K.J. Wong, D.E. Milenic, P.L. Choyke, M.W. Brechbiel, Mol. Pharm. 5 (2008) 527–539.
[6] A.J. Villaraza, A. Bumb, M.W. Brechbiel, Chem. Rev. 110 (2010) 2921–2959.
[7] Y.H. Bae, K. Park, J. Control. Release 153 (2011) 198–205.
[8] J.A. Park, J.J. Lee, J.C. Jung, D.Y. Yu, C. Oh, S. Ha, T.J. Kim, Y. Chang, ChemBioChem 9 (2008) 2811–2813.
[9] P.C. Brooks, R.A. Clark, D.A. Cheresh, Science 264 (1994) 569–571.
[10] R. Haubner, D. Finsinger, H. Kessler, Angew. Chem. Int. Ed. Engl. 36 (1997) 1374–1389.
[11] J.P. Xiong, T. Stehle, R. Zhang, A. Joachimiak, M. Frech, S.L. Goodman, M.A. Arnaout, Science 296 (2002) 151–155.
[12] R. Haubner, Eur. J. Nucl. Med. Mol. Imaging 33 (2006) S54–S63.
[13] Y. Zhou, S. Chakraborty, S. Liu, Theranostics 1 (2011) 58–82.
[14] F. Danhier, A.L. Breton, V. Preat, Mol. Pharm. 9 (2012) 2961–2973.
[15] G. Casiraghi, G. Rassu, L. Auzzas, P. Burreddu, E. Gaetani, L. Battistini, F. Zanardi, C. Curti, G. Nicastro, L. Belvisi, I. Motto, M. Castorina, G. Giannini, C. Pisano, J. Med. Chem. 48 (2005) 7675–7687.
[16] L. Auzzas, F. Zanardi, L. Battistini, P. Burreddu, P. Carta, G. Rassu, C. Curti, G. Carsiraghi, Curr. Med. Chem. 17 (2010) 1255–1299.
[17] J.-A. Park, Y.J. Lee, J.W. Lee, K.C. Lee, G.I. An, K.M. Kim, B.I. Kim, T.-J. Kim, J.Y. Kim, ACS Med. Chem. Lett. 5 (2014) 979–982.
[18] S. Achilefu, H.N. Jimenez, R.B. Dorshow, J.E. Bugaj, E.G. Webb, R.R. Wilhelm, R. Rajagopalan, J. Johler, J.L. Erion, J. Med. Chem. 45 (2002) 2003–2015.
[19] S. Achilefu, R.B. Dorshow, J.E. Bugaj, R. Rajagopalan, Invest. Radiol. 35 (2000) 479–485.
[20] Z.B. Li, K. Chen, X. Chen, Eur. J. Nucl. Med. Mol. Imaging 35 (2008) 1100–1108.
[21] S. Liu, Z. Liu, K. Chen, Y. Yan, P. Watzlowik, H.J. Wester, F.T. Chin, X. Chen, Mol. Imaging Biol. 12 (2010) 530–538.
[22] L.M. De León-Rodríguez, K. Zoltan, Bioconjug. Chem. 19 (2008) 391–402.
[23] Y. Wu, X. Zhang, Z. Xiong, Z. Cheng, D.R. Fisher, S. Liu, S.S. Gambhir, X. Chen, J. Nucl. Med. 46 (2005) 1707–1718.
[24] X. Zhang, Z. Xiong, Y. Wu, W. Cai, J.R. Tseng, S.S. Gambhir, X. Chen, J. Nucl. Med. 47 (2006) 113–121.
[25] M. Schottelius, H.U. Wester, Methods 48 (2009) 161–177.
[26] J. McConathy, M.M. Goodman, Cancer Metastasis Rev. 27 (2008) 555–573.